Cell Reports Medicine, Volume *4*

Supplemental information

Synergistic effects of combined immunotherapy strategies in a model of multifocal hepatocellular carcinoma

Maria Carmen Ochoa, Sandra Sanchez-Gregorio, Carlos E. de Andrea, Saray Garasa, Maite Alvarez, Irene Olivera, Javier Glez-Vaz, Carlos Luri-Rey, Iñaki Etxeberria, Assunta Cirella, Arantza Azpilikueta, Pedro Berraondo, Josepmaria Argemi, Bruno Sangro, Alvaro Teijeira, and Ignacio Melero

Sup. Fig 1

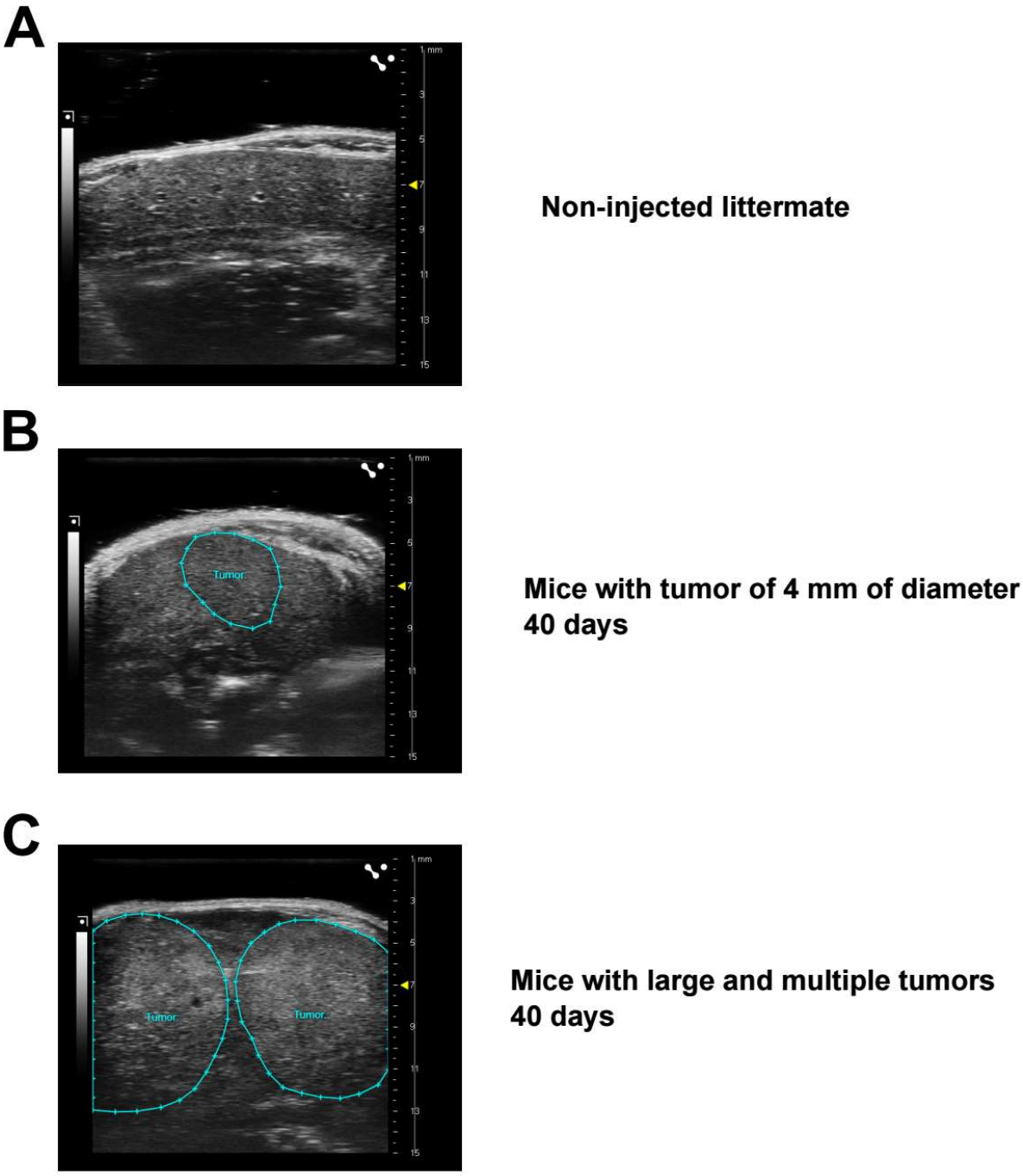

Supplementary figure 1. Ultrasound exams may monitor tumor progression in the model. Examples of abdominal ultrasound scans of HCC tumors and liver imaging of a non-injected healthy littermate mouse as a control. See also figure 1.

Sup. Fig 2

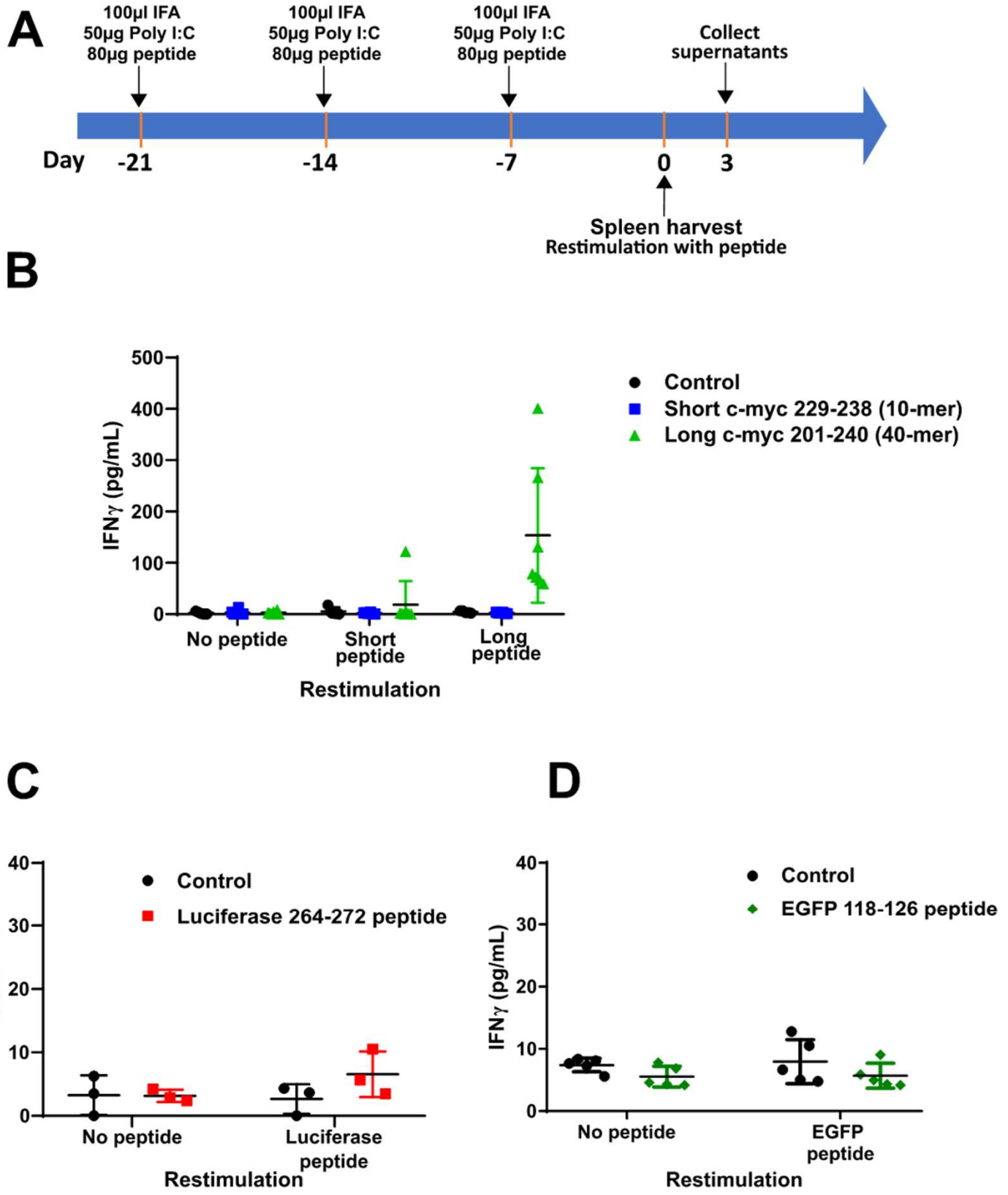

Supplementary figure 2. Weak but detectable immunogenicity of human c-myc and luciferase in mice. (A) Scheme of immunization with described c-myc, luciferase and EGFP peptides in the indicated (IFA + poly I:C) adjuvant[19-21]. Splenocytes recovered on day 0 were restimulated in vitro and the supernatants of 72h-cultures were assayed for IFNγ concentrations. (B) Response to immunogenic human c-myc peptides in C57Bl/6 mice. (C and D) Similar experiments with reported immunogenic peptides of luciferase and EGFP that gave weak or none reactivity in the intensively immunized mice. See also figure 1.

Sup. Fig 3

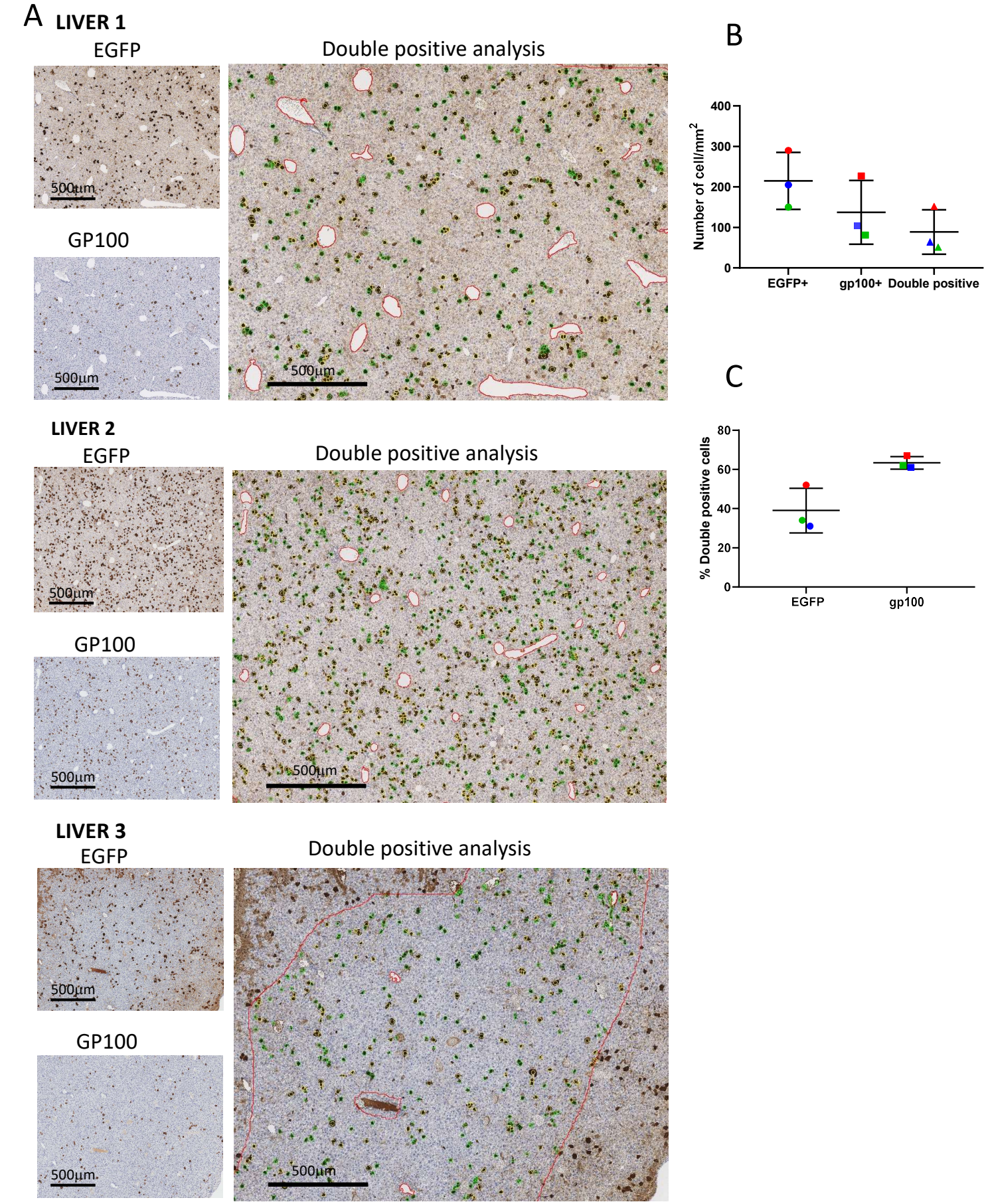

Supplementary figure 3. Efficiency of simultaneous transgene expression upon hydrodynamic gene transfer. (A) Representative images IHC serial precisely overlapped sections stainings for EGFP and gp100 and the double positive analyses from mouse livers given the combination plasmids. Red line marks excluded areas to avoid edge effect. EGFP single positive cells are depicted in green and double positive are yellow. (B) Density of single positive and double positive hepatocytes. (C) Percentage of the double positive cells among those which are $EGFP^{+}$ or $gp100^{+}$. See also figure 1.

Sup. Fig 4

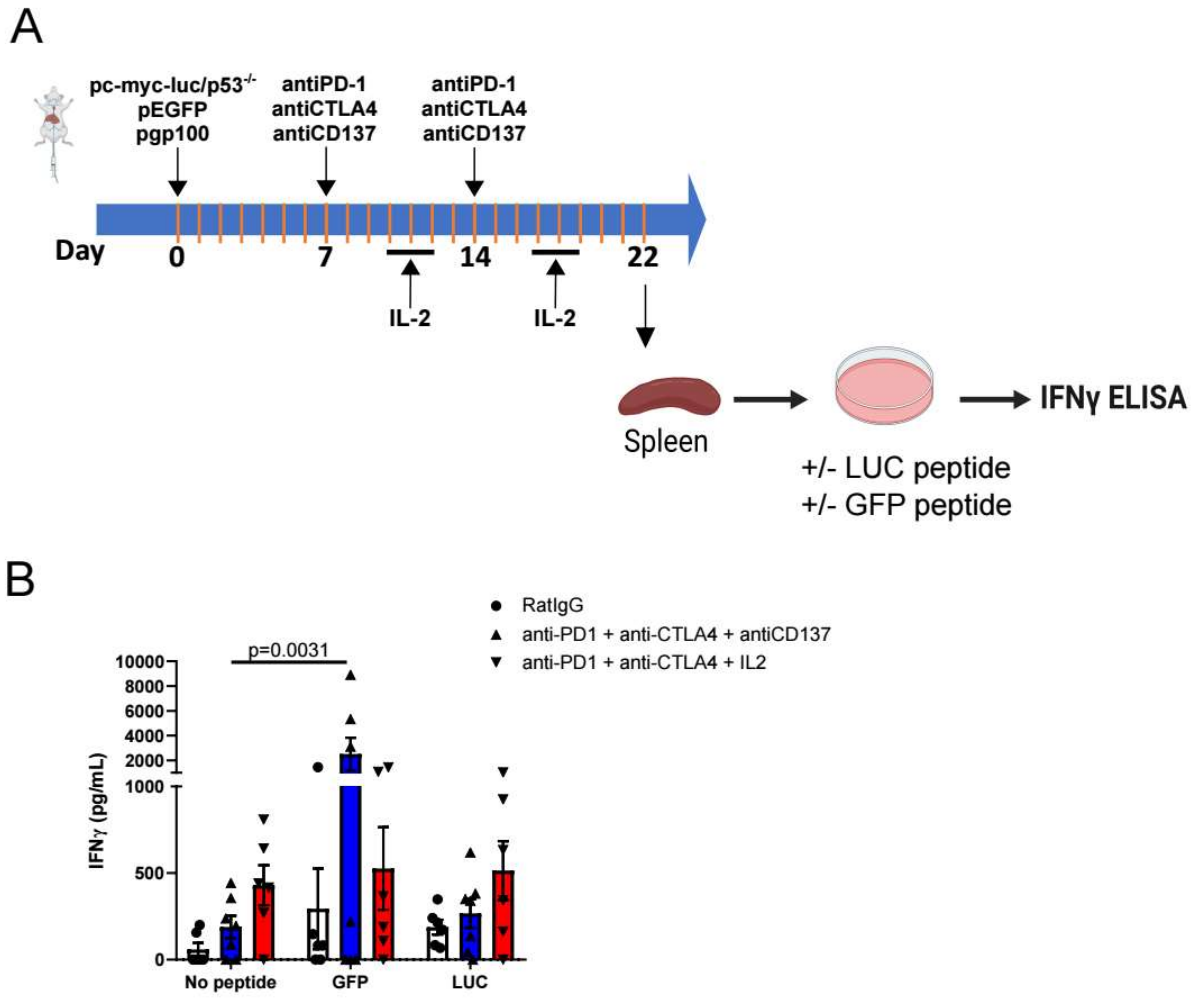

Supplementary figure 4. Ex vivo IFNγ production by splenocytes from mice gene-transferred with plasmids c-myc-luc, p53$^{-/-}$, pSB13, pGFP and pgp100 restimulated with luciferase and GFP peptides. (A) Scheme of the experiments (B) Each point represents data from one mouse. Statistical comparison were calculated with two-way ANOVA. See figure 2.

Sup. Fig 5

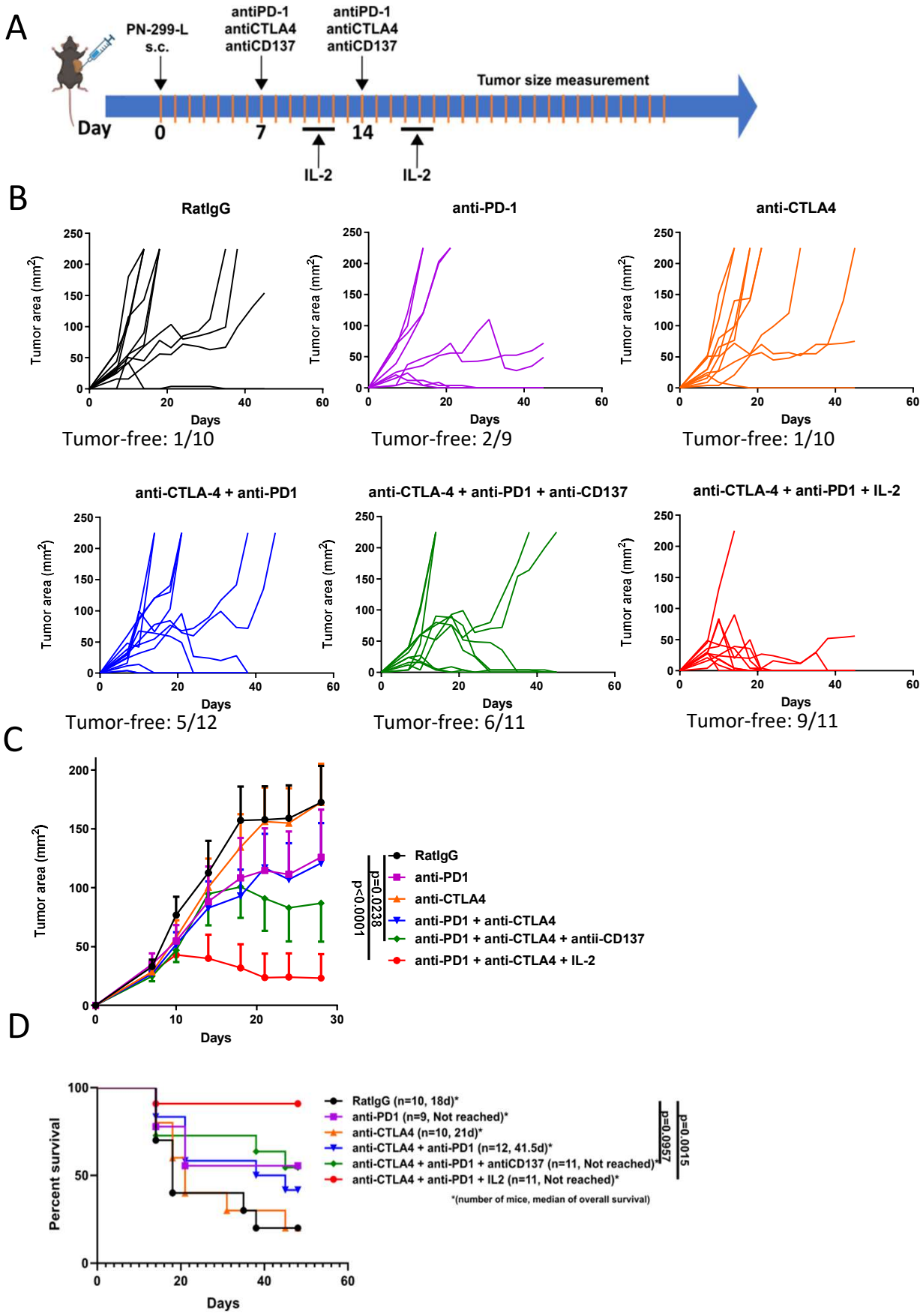

Supplementary figure 5. Antitumor efficacy of the combined immunotherapy treatments on subcutaneous tumors derived from the PN-299-L cell line. (A) Schematic representation of the experiment time course and follow-up of tumor sizes. (B) Individual tumor size follow-up of the groups of mice given the indicated treatments. Fractions of mice tumor-free at the end of the experiment are provided. (C) Statistical comparisons. (D) Overall survival with the numbers of mice for group and the median overall survival for each treatment group. This experiment has been replicated twice with similar results. See also figure 2.

Sup. Fig 6

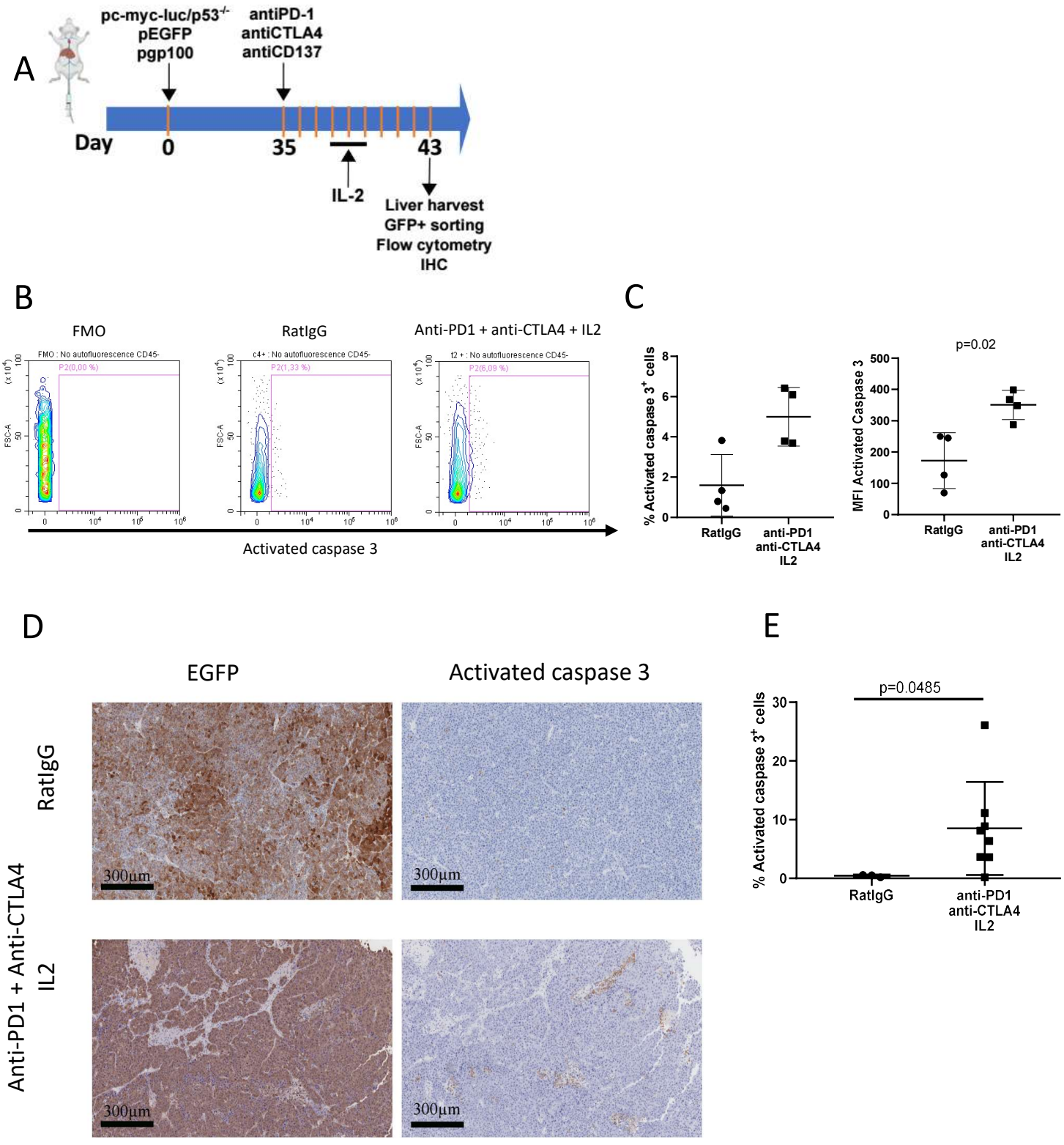

Supplementary figure 6. Apoptosis *in vivo* induction of EGFP⁺ hepatocytes upon triple treatment with anti-PD1 + anti-CTLA4 + IL2. (A) Experimental scheme in which mice were treated as indicated and livers retrieved on day 43 FACS-sort EGFP⁺ cells from cell suspensions to be studied by flow cytometry and to be fixed and paraffin embedded for IHC analyses. (B) Activated caspase 3 intracellular staining of EGFP⁺ sorted hepatocellular carcinoma cells. (C) Quantitative data corresponding to 4 individual livers from mice under triple treatment or treated with control antibody. (D) Serial sections stained for EGFP and cleaved caspase 3. Representative images are shown for the treatment and control groups. (E) Compiled quantitative data from 8 livers corresponding to each experimental group. See figure 7.